



Dmytro Gryn^{1,*}, Oleksandr Liashchuk², Yurii Otruba³, Yuriy Andrushchenko²

¹ S. I. Subbotin Institute of Geophysics of the National Academy of Sciences of Ukraine, Kyiv, 03142, Ukraine

² The Main Center of Special Monitoring, State Space Agency of Ukraine, Gorodok, 12265, Ukraine

³ State Institution National Antarctic Scientific Center, Ministry of Education and Science of Ukraine, Kyiv, 01601, Ukraine

* Corresponding author: gryn.dmytro@ukr.net

The impact of surface waves of South American earthquakes on the ice sheet of the Antarctic Peninsula

Abstract. Earthquakes cause fluctuations in the surface of the geological environment, which may affect Antarctica's ice sheet. As seismic waves interact with a glacier, more fissures appear, and its speed may increase. These processes may accelerate the reduction in the total mass of the West Antarctic ice cover. We analysed the physical impact of earthquakes registered at the Ukrainian Antarctic Akademik Vernadsky station on some local glaciers. We also aimed to indirectly identify the consequences of the destruction of the integrity of the glacier structure, which are accompanied by the appearance of induced seismicity. The most characteristic wave fields from various seismically active tectonic zones around Galindez Island were selected to analyse glacier response to earthquake-related seismic forces. We analysed the acceleration of the ground's surface for short-term earthquakes and the time during which these seismic waves were acting on the local glaciers. Seismic data from the most distant earthquake in Peru, magnitude 7.2, which occurred on May 26, 2022, at 12:02:21 UTC, were used to avoid the cumulative effect of P waves, S waves, and surface waves. Seismic waves of different types arrive at the observation point at different times due to the large distance from the source and different rates of wave propagation. This separation allows us to study the interaction of each type of wave and the glacier individually. This publication reports our analysis of the effect of a long-period surface wave on glaciers near Galindez Island. Induced cryoseismicity manifests itself in the high-frequency region of seismic records as a series of pulses associated with the formation of ice cracks. We used the data from the Guralp CMG 40-TDE seismic station is currently the only one at the Akademik Vernadsky station. The available seismic data made it possible to identify the cause-and-effect relationship between teleseismic waves from tectonic earthquakes and local cryoseismicity. However, the data from a single station do not allow for locating cryoseismic sources. We also analysed the characteristic local interference wave fields that complicate detecting target waves.

Keywords: cryoseismics, glaciers, magnitude, seismology

1 Introduction

Climatological factors are considered the main reason for the decrease in the volume of Antarctica glaciers. These factors are increasing temperatures of the ocean currents that reach the continent and of the warming atmospheric air masses above it. In contrast to East Antarctica, the snow

and ice cover in West Antarctica does not recover over the winter (Paolo et al., 2015; Davison et al., 2023). Geological and geophysical phenomena also affect the stability of the Antarctic cryosphere.

The study, set in West Antarctica, considers how the high-energy seismic wave fields created by earthquakes affect glaciers. The waves can accelerate the glacier's motion and promote ice fracturing.

The fracturing of the near-surface ice occurs during volumetric deformation (compression-extension) at the passage of high-amplitude seismic waves.

Such a natural phenomenon was strongly confirmed by seismic records of the Chilean earthquake of 2010 (magnitude 8.8), collected during large-scale international projects POLENET (The Polar Earth Observing Network) and AGAP (Antarctica's Gamburtsev Province Project) monitoring the central part of Antarctica. Over 40 temporary seismic stations were installed there in 2007–2011. Researchers of the Georgia Institute of Technology, USA (Walter et al., 2013; Peng et al., 2014) state that the Antarctic permafrost is sensitive to surface seismic waves even from very distant earthquakes.

We aimed to analyse seismic data registered at the Akademik Vernadsky station and to search for high-energy Rayleigh and Love surface waves generated by nearby and distant earthquakes. We also aimed to determine what occurs in glaciers during their interaction with surface waves and for a while afterwards. In particular, we aimed to detect high-frequency seismic pulses resulting from the nucleation of cracks (ruptures) due to short-period harmonic oscillations and volume deformation. Finally, we aimed to quantitatively describe the induced cryoseismic events that manifest in the changes in the ice cover of the islands close to the research station.

Reviews of glacier seismology (Aster & Winberry, 2017; Ringler et al., 2022) note the contribution of Zhigang Peng and Jacob I. Walter in the identification and research of the earthquakes' destructive action on the Antarctic glaciers.

Li et al. (2021) provide the results of a multi-year study of remotely-induced microseismic activity around Mt. Erebus on Ross Island; most short-period cryoseismic events happened during the passage of Rayleigh waves induced by the earthquakes.

As the logistics of a comprehensive long-term seismic monitoring of Antarctic glaciers is immensely complicated, scientists turn to experimental alternatives. One way to do this is to con-

duct a series of artificial seismic works on the surface of a frozen water reservoir (Xie et al., 2024). The authors induced vibrations representative of an earthquake and so studied how the seismic waves spread in the ice and how the ice plate is destroyed.

Su and Liu (2019), McBrearty et al. (2020), and Jennings and Hambrey (2021) also studied spatio-temporal deformations inside glaciers caused by seismic waves and causing, in their turn, secondary seismicity. One way to simulate ice deformation is by using the finite element method.

The earthquakes' effect on the mountain glaciers is reviewed by Li et al. (2022), Liu et al. (2022), and Li et al. (2023). The articles determine the degree of glaciers' damage, increased mobility, and the dangers to people and infrastructure these effects create.

Section 2 describes the equipment used to obtain the seismological data and the geographical location of the three seismoactive territories where the earthquakes' hypocenters were. To interpret the seismological data and determine the effect of seismic waves on the glaciers, we used spectral analysis (time-frequency and amplitude-frequency). We identified seismic signals typical for earthquakes and other seismicity of various origins. Section 3 presents the results of identifying groups of identical (in terms of amplitude-frequency parameters) seismic waves related to cracks forming in the glaciers as surface waves related to the Chilean earthquake passed through them. The glaciers' induced seismicity appears due to high-amplitude volumetric movements of compression and extension. Section 4 discusses the identification of seismic cryoevents and focuses on the impossibility of pinpointing their exact locations, as the Ukrainian Antarctic Akademik Vernadsky station has only one seismic station. To identify the precise site and the origin mechanisms of cracks, at least three such stations should monitor the glacier. Despite the complications of long-term seismic measurements in the region, we found new details of the earthquakes' impact on the glaciers. The conclu-

sions in Section 5 confirm other researchers' findings on the role of earthquakes in hastening the retreat of glaciers and the reduction of the ice masses in Antarctica.

2 Materials and methods

The publication uses the results of interpreting three-component seismological records of the Guralp CMG 40-TDE velocimeter of the Akademik Vernadsky station. The recording frequency range of 0.033 to 50.0 Hz accommodates low- and high-frequency events. Seismograms of wave fields generated by earthquakes and by the impact of the earthquakes on the cryosphere were used. The time interval is set by the first and the last arrivals of seismic waves. Usually, it depends on the distance to the hypocenter — the more distant the earthquake, the longer the record. The main types of seismic waves used for the analysis are low-frequency Rayleigh and Love surface waves and high-frequency pulses at the transition of potential energy to kinetic energy when the glacier cracks. We also studied other types of signals, considered as aftereffector interference waves.

To time the earthquakes and find their precise hypocenter depths, publicly available data on seismic events from the USGS website (United States Geological Survey, <https://earthquake.usgs.gov/>) were used.

To time the first arrival of a seismic wave and to find their true physical properties, polarization analysis — a mathematical tool for processing discrete time functions — was used. A seismic wave type was also determined with the help of polarization analysis — P (primary), S (secondary), and Rayleigh and Love surface waves (Pinnegar, 2006; Greenhalgh et al., 2018; Brinkman et al., 2023).

Power spectrum (amplitude-frequency) analysis and time-frequency analysis are two methods used to analyse signals in the frequency domain. They are used to search for regularities that explain seismic natural phenomena and their effects on the environment. Time-frequency anal-

ysis can detect a weak nonlinear regularity from random noise-like and chaotic oscillatory signals. This mathematical tool makes it possible to separate and remove overlapping events of different genesis in the spectral domain.

Power spectrum analysis provides information about the distribution of power in a signal over different frequencies. It is typically used to analyse stationary signals, where the signal's frequency content does not change over time. Time-frequency analysis, on the other hand, is used to analyse non-stationary signals. It provides information about how the distribution of power in a signal over different frequencies changes over time. This is achieved by dividing the signal into short segments and analysing each segment separately using power spectrum analysis (Båth, 1974; Wang, 2022).

2.1 Territories of seismic influence on the Antarctic Peninsula

The nearest active seismic zone is up to 180 km in the southeast direction from the Akademik Vernadsky station (Fig. 1). The epicenters of the earthquakes are located on the surface of the Shetland Plate and extend along the South Shetland Trough, parallel to the Antarctic Peninsula. It is considered the only tectonically active part of the Antarctic continental margin (Reading, 2007; Feenstra et al., 2019). According to Yegorova et al. (2011) and Civile et al. (2012), the oceanic lithosphere subducts here under the continental crust of the Antarctic Peninsula. During the period of active observations, 77 earthquakes of magnitude 3 to 5 and about 50 earthquakes of magnitude 5 to 7 were identified here. Most occur at a depth of about 5 to 12 km above ocean level (Smalley et al., 2021).

The Antarctic Peninsula has few earthquakes with magnitudes of 4–5 that occur at depths of up to 15 km. To the southwest of the Antarctic Peninsula is a part of the Antarctic Plate where earthquakes of magnitude 4–5 are observed at depths of up to 12 km. In 1998, a strong earthquake (magni-



Figure 1. The location of the epicenters of earthquakes (gray circles) in the southeastern part of the seismically active territories, which were registered at the Akademik Vernadsky station (red circle) during the wintering of the 27th Ukrainian Antarctic Expedition 2022–2023. Green circles show the seismoactive regions (numbers 1, 2, and 3 refer to the sequence of the region's description in the text)

tude 8.1) occurred in the oceanic plate near the Balleny Islands (Tsuboi et al., 2000; Sykes, 2021).

The Scotia plate is located 800 km from the Akademik Vernadsky station, between the South American and Antarctic plates (Fig. 1). At the points of contact of these three plates, seismically active Southern and Northern ridges formed (Govers et al., 2021), which are part of the Pacific seismic belt. From the eastern side of the Scotia plate, the seismically active Sandwich microplate is separated, formed by the subduction of the South American plate (van de Lagemaat et al., 2021; Jia et al., 2022). The sinking rate is 65–78 mm per year (Cannata et al., 2017). According to the

NEIC (National Earthquake Information Center) global earthquake bulletin (U.S. Geological Survey), from 1921 to 2023, approximately 2 600 seismic events with a magnitude greater than 5 occurred here. On August 12, 2021, two earthquakes occurred under the Sandwich microplate with a magnitude of 7.5 and 8.2 (Giner-Robles et al., 2009). Most earthquakes occur at depths of up to 200 km. This tectonic activity makes this site unique for study, as such powerful seismic events can cause secondary effects such as seismicity in non-seismic areas, tsunamis, and coastal ice sheet collapse.

At a distance of 2500 to 5500 km from the station in the northern direction, there is an elongated area with regular seismic events that occur on the border of the Nazca and South American tectonic plates (Fig. 1). At this point, the Nazca plate is subducting under the South American plate at a rate of 80 mm per year (Schepers et al., 2017). During strong earthquakes, the submergence can reach 18 meters at a time. Here, in 1960, the most powerful earthquake ever was registered, with a magnitude of 9.6 (Stein et al., 1986).

2.2 Seismic events recorded by the Guralp CMG 40-TDE velocimeter

At the Akademik Vernadsky station, ground oscillations are recorded with a Guralp CMG 40-TDE velocimeter. The direction of the ground movement is determined in the three-dimensional space by two horizontal sensors (HHE (High-Broadband and High-gain seismometers), oriented to the East, and HHN, oriented to the North) and one vertical sensor. These ground motions arise from many different sources and are caused by the interaction of various objects with the Earth's surface and the internal tectonic motions. Earthquakes occurred in different geological structures at different distances from the station and had different magnitudes and hypocenter depths. Below are selected the most characteristic seismograms from earthquakes of the main tectonically active structures of the northeastern section tangential

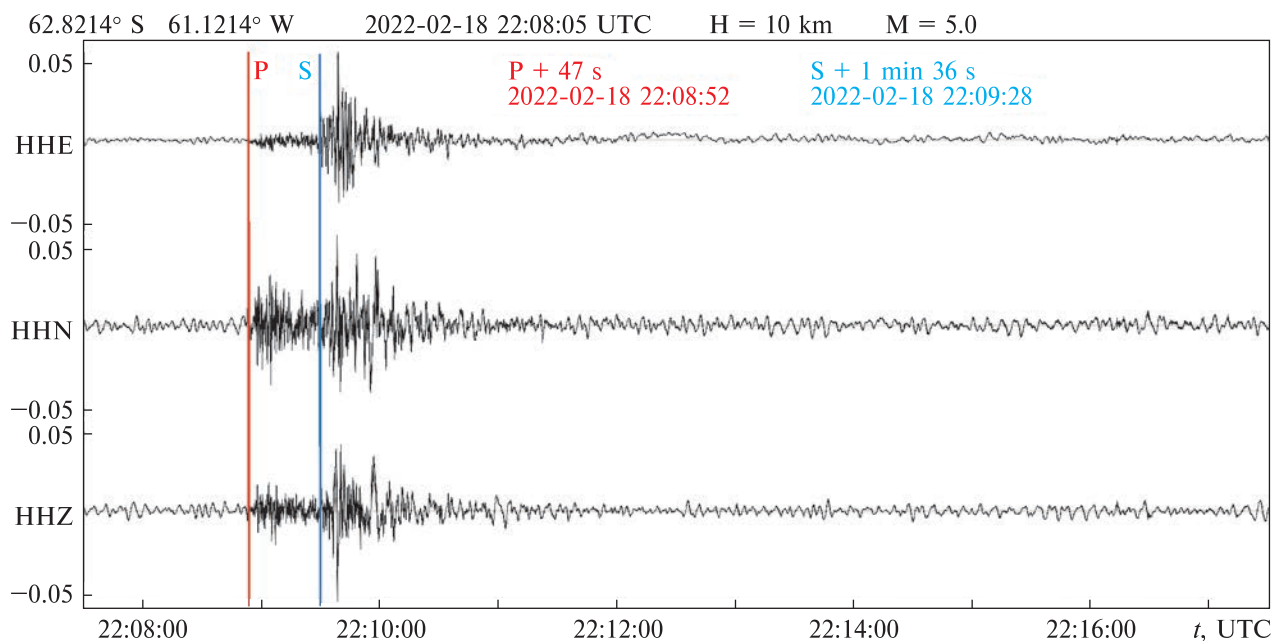


Figure 2. Three-component recording (HHE, HHN, HHZ) of the Earth's surface oscillations from the Shetland earthquake on Galindez Island. The length of time for recording the three components is 5 minutes. The vertical scale shows the amplitude of the oscillation of the Earth's surface at the point of observation (in millimeters). The horizontal axis shows the time of registration of seismic waves. H – focal depth of earthquake, M – magnitude

to the Antarctic Peninsula: Antarctic, South American, Nazca, Shetland, Scotia, Sandwich plates, and South and West Scotia ridges.

2.2.1 Shetland earthquake

During the wintering of the 27th Ukrainian Antarctic Expedition, on the Shetland plate and the southern ridge of Scotia, more than a dozen earthquakes with a magnitude greater than 4 occurred. One of the closest earthquakes to the station, with a magnitude of 5.0, was registered at 22:8:52 UTC (Greenwich Mean Time) on February 18, 2022 (green circle 1 in Fig. 1). The coordinates of the epicenter of the earthquake are 62.8214°S, 61.1214°W, time of occurrence 2022-02-18 22:08:05 UTC, hypocenter depth – 10.0 km. It took place in the southwestern part of the South Shetland Islands, 325 km from the station. The longitudinal wave reached Galindez Island 47 seconds after the earthquake, and the transverse wave after 1 minute 36 seconds. A feature of the seismic

records of the earthquake from this region is the weak amplitude of the oscillation of the HHE component (Fig. 2).

Galindez Island was under the influence of seismic waves from the earthquake for 3 minutes. The main part of the energy is in the transverse S wave of 0.1 to 1.0 Hz. The longitudinal wave has higher-frequency harmonics, from 0.8 to 20.0 Hz (Fig. 3). The amplitude-frequency spectrum shows the amplitude-dominant harmonics of seismic waves.

2.2.2 Sandwich earthquake

On the Southern Sandwich Islands (58.7479°S, 26.0934°W) located 2013 km from the station, an earthquake with a magnitude of 6.3 and a hypocenter depth of 78.0 km occurred on 2022-10-25 at 00:13:01 UTC.

Due to the large distance between the point of generation of seismic waves and the point of observation, the main waves were separated in time.

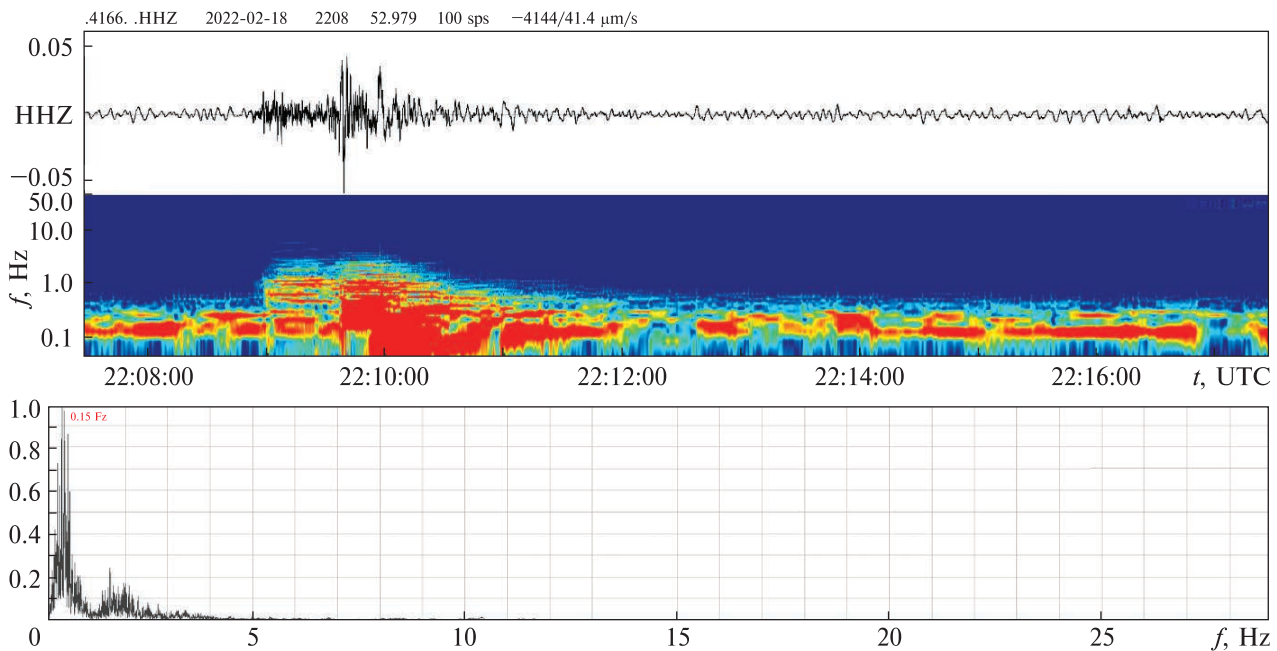


Figure 3. Seismogram of the vertical HHZ component of the Shetland earthquake (top panel). Time-frequency (middle panel,) distribution of power spectral density in logarithmic scale (color scale in dB relative units mm/Hz). The same color scale in the panels in Figures 5, 6, 8, 9, 10, 11. A bottom panel is amplitude-frequency distribution of energy of vibration of the Earth's surface (Normalized power, dB)

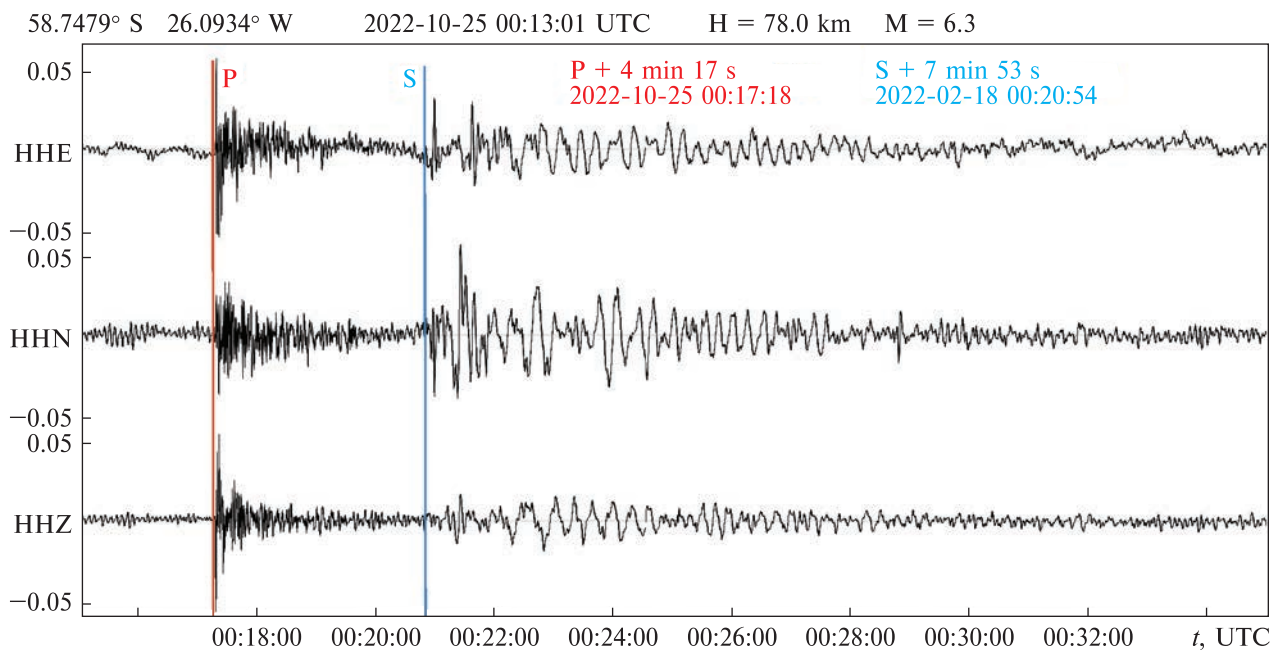


Figure 4. Three-component seismic records (HHE, HHN, HHZ) of the Sandwich earthquake on Galindez Island. The vertical axis shows the amplitude of the oscillation of the Earth's surface (in millimeters). The horizontal axis shows the time of registration of seismic waves

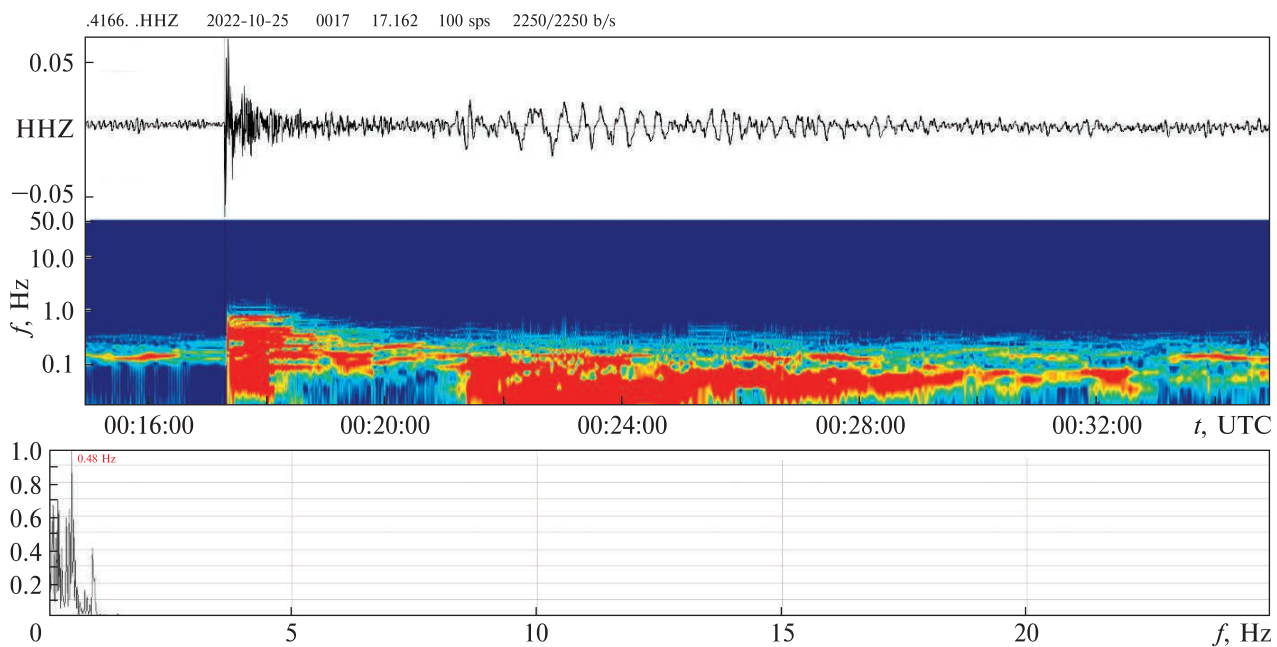


Figure 5. Seismogram of the vertical HHZ component of the Sandwich earthquake. Time-frequency (logarithmic scale) and amplitude-frequency distribution of the energy of vibration of the Earth's surface

In fact, the slower, lower-frequency S wave is recorded after the ground surface has finished oscillating from the faster, higher-frequency P wave. The time difference between them, according to Figure 4, is 3 min 36 sec. The longitudinal wave traveled a distance of 2013 km in 4 minutes and 17 seconds; its average speed during this interval was $7.382 \text{ km} \cdot \text{s}^{-1}$. The speed of the transverse wave was $4.256 \text{ km} \cdot \text{s}^{-1}$. The epicenter is marked by green circle 2 in Figure 1.

Galindez Island was under the influence of seismic waves from the earthquake for 7 minutes. The amplitude-frequency spectrum shows the amplitude-dominant harmonics of seismic waves (Fig. 5). The longitudinal wave consists mainly of high-frequency harmonics (from 5.0 to 30.0 Hz). Its amplitude maximum is in the range of 10.0–14.0 Hz. The main part of the energy in the transverse S wave is carried by 0.1 to 5.0 Hz.

A feature of the seismic record of the Sandwich earthquake is the presence of frequencies up to 0.2 Hz during the next 30 minutes after the passage of transverse and longitudinal waves. These

low-frequency waves are absent at 00:00:00 – 00:17:18, before the earthquake, and present at 00:30:00 – 01:00:00 (Fig. 6), after it.

2.2.3 Peruvian earthquake

An earthquake occurred in Peru (14.8942°S , 70.1969°W), 5620 km from the station, on 2022-05-26 at 12:02:21 UTC. The depth of the hypocenter was 252.0 km, and the magnitude was 7.2. Its position is marked by green circle 3 in Figure 1.

The distance of more than 5500 km between the epicenter of the earthquake and the station contributed to the main types of waves' separation in time. Figure 7 shows seismograms of the two horizontal components, HHE and HHN, and the vertical HHZ. The time difference between the higher-frequency P wave and the lower-frequency S wave, according to Figure 7, is 6 min 27 sec. The longitudinal wave traveled a distance of 5620 km in 8 min 34 sec; its average speed during this interval was $10.933 \text{ km} \cdot \text{s}^{-1}$. The transverse wave traveled a distance of 5620 km in

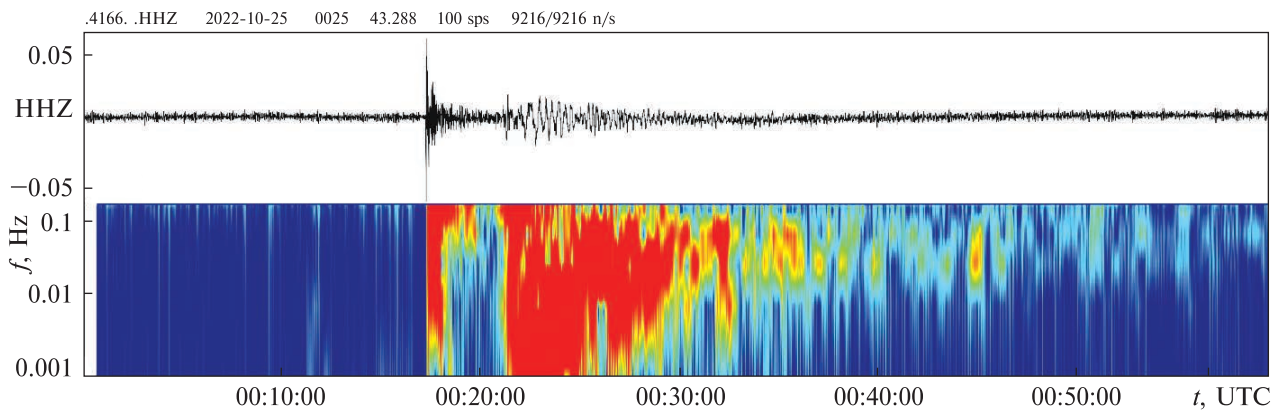


Figure 6. Time-frequency (logarithmic scale) energy distribution of the vertical component of the seismic record from the Sandwich earthquake in the low-frequency range of 0.001–0.1 Hz

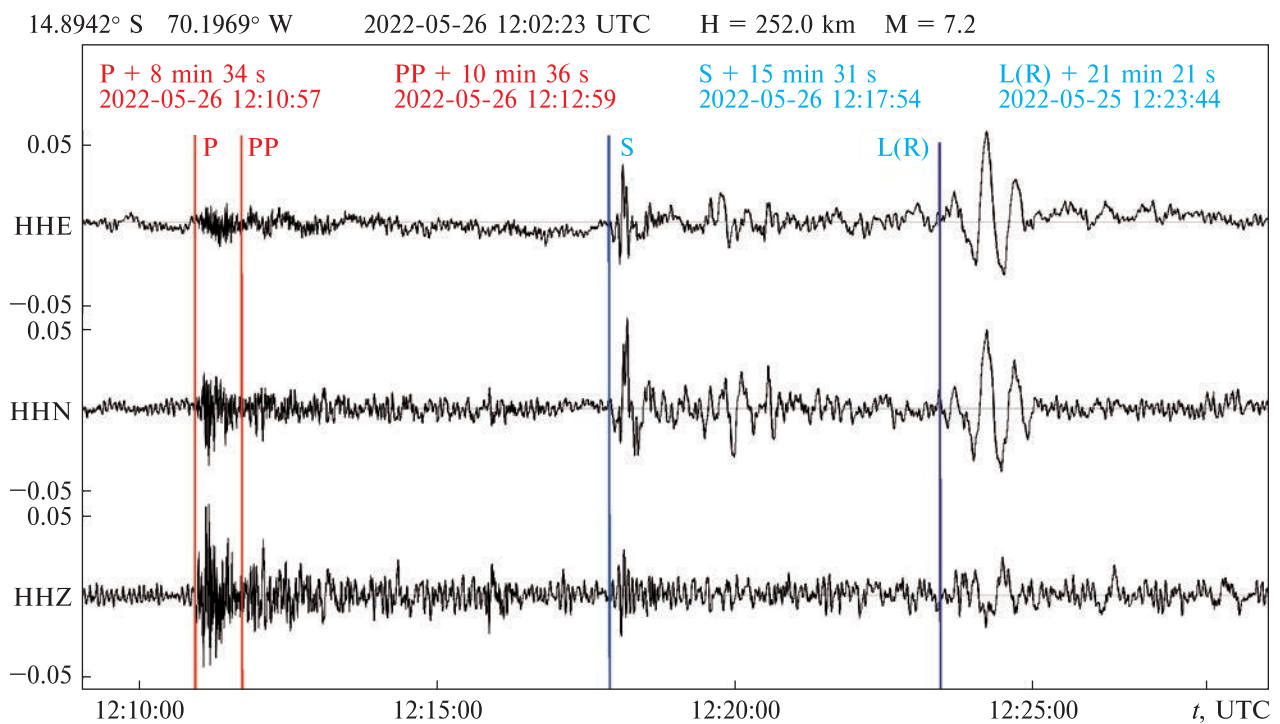


Figure 7. The three-component amplitude data (HHE, HHN, HHZ) recorded at the Akademik Vernadsky station from the Peruvian earthquake covers more than 20 minutes. The vertical axis shows the amplitude of the oscillation of the Earth's surface at the point of observation (in millimeters). The horizontal axis shows the time of registration of seismic waves

15 min 31 sec; its average speed during this interval was $6.037 \text{ km} \cdot \text{s}^{-1}$.

In the Shetland and Sandwich earthquakes, the surface waves were too weak to be separated from

the general wave field and were complicated by S waves. In the wave field of the Peruvian earthquake, in addition to the P and S waves, the surface wave L(R) stands out well, as it is distant and

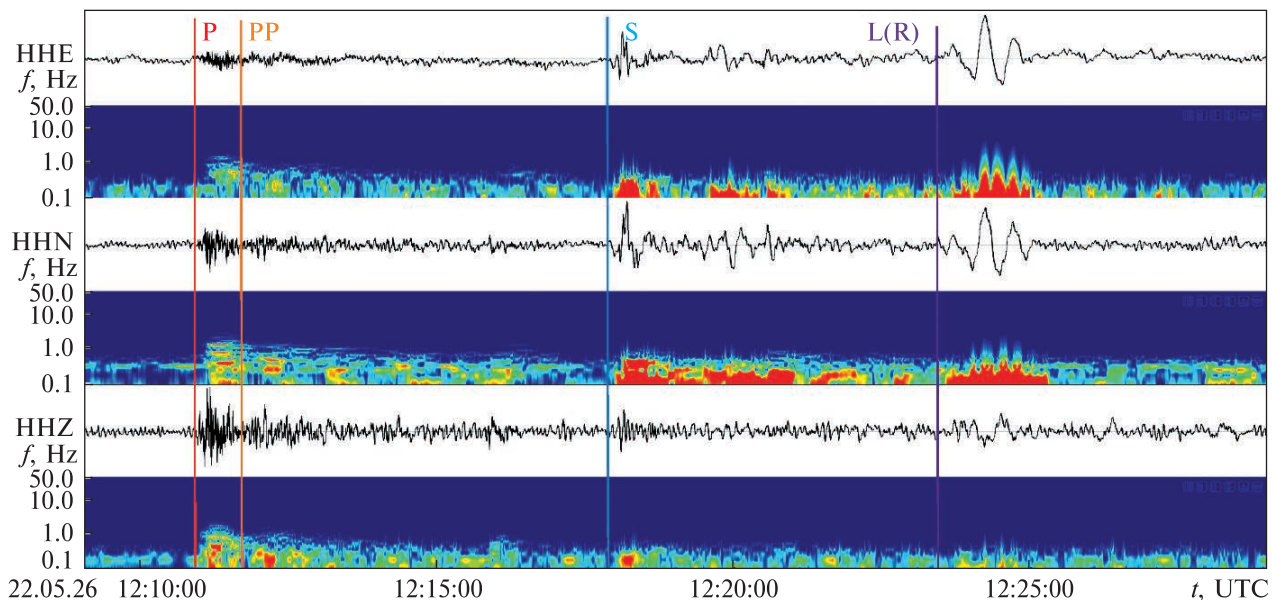


Figure 8. A three-component transcript (HHE, HHN, HHZ) of the Earth's surface oscillation amplitude from the Peruvian earthquake recorded on Galindez Island and the respective time-frequency (logarithmic scale) spectra

clearly separated from other waves. It has a large amplitude in the horizontal components (HHE, HHN), many times greater than P and S waves. The average calculated speed of the surface wave is $4.387 \text{ km} \cdot \text{s}^{-1}$.

A three-component seismogram with the respective time-frequency spectra is shown in Figure 8. It can be seen that oscillations with frequencies characteristic of an earthquake are registered on Galindez Island for more than 18 minutes after the arrival of the first P wave. As with earthquakes from other seismically active zones, the longitudinal wave has a higher frequency than the transverse. The surface wave is recorded for 90 seconds. The vectors of low-frequency oscillations (Fig. 8) of transverse and surface waves lie in the horizontal plane. This is an important consideration for the further study of how earthquakes affect Antarctic glaciers.

2.3 Wave interference

A series of seismic oscillations from stochastic events must be classified as interference or noise for the correct solution to a certain problem. They

significantly complicate seismic records and reduce the reliability of interpretation. Often, useful seismic events and disturbances have the same spectral composition, making their separation and classification impossible. For example, Figure 9 shows a ten-minute seismogram without seismic waves characteristic of earthquakes. In the frequency range of 0.1–20.0 Hz, almost the same amplitude of harmonic oscillation is observed throughout the entire time interval. These noises have a different nature, and for certain tasks, they carry useful information. The frequency range from 20.0 to 50.0 Hz is not displayed due to the low-frequency component's multiple energy (amplitude) dominance.

As mentioned above, high-frequency harmonics of random oscillations received by our station carry information mainly about non-tectonic events. For their detection, we applied filters to remove frequencies from 0 to 5.0 Hz, which are characteristic both for earthquakes and for a number of meteorological phenomena (Anthony et al., 2015). Figure 10 shows a seismic record of the vertical HHZ component, which has a spectral compo-

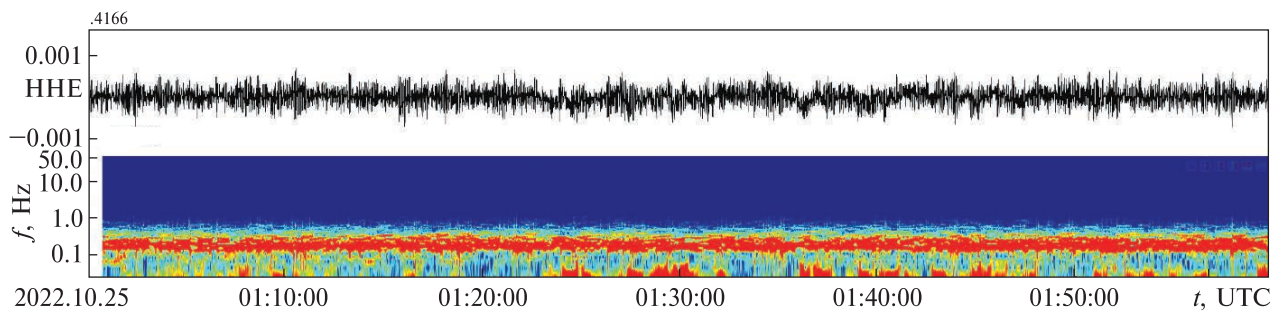


Figure 9. Seismogram of the NNZ vertical component with a recording of seismic noise and its time-frequency distribution of seismic wave energy

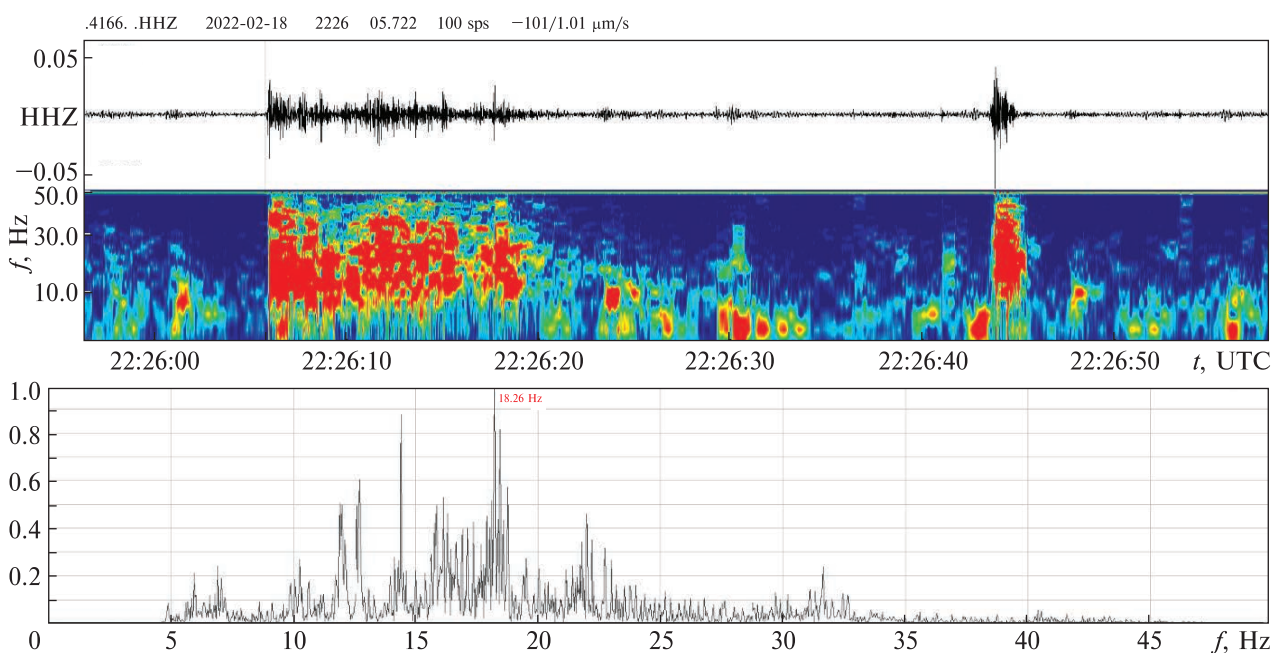


Figure 10. Seismogram of the vertical HHZ component (0–50.0 Hz) with non-seismological events. High-frequency components of the time-frequency and amplitude-frequency spectra of the seismic recording at the Akademik Vernadsky station

sition in the range of 0.5–50.0 Hz. It records two events.

The first has a clearly defined beginning, temporal variability in interaction with the Earth's surface, activity for 15 seconds, and a gradual decrease. The second event lasted for about 2 seconds. The amplitude-frequency characteristics of these events have identical spectra and probably the same origin. It can be assumed that they are caused by the breaking of the ocean ice cover (ice)

against the island's coastline or their interaction caused by the wind. Such events and their intensity will vary throughout the day and are seasonal. Temporal coincidence of the waves from an earthquake and this class of events will cause a significant error in the local magnitude of the earthquake. One of the ways to detect noise is to use statistics on the directions of the arrival of waves from sources of various seismically active geological objects.

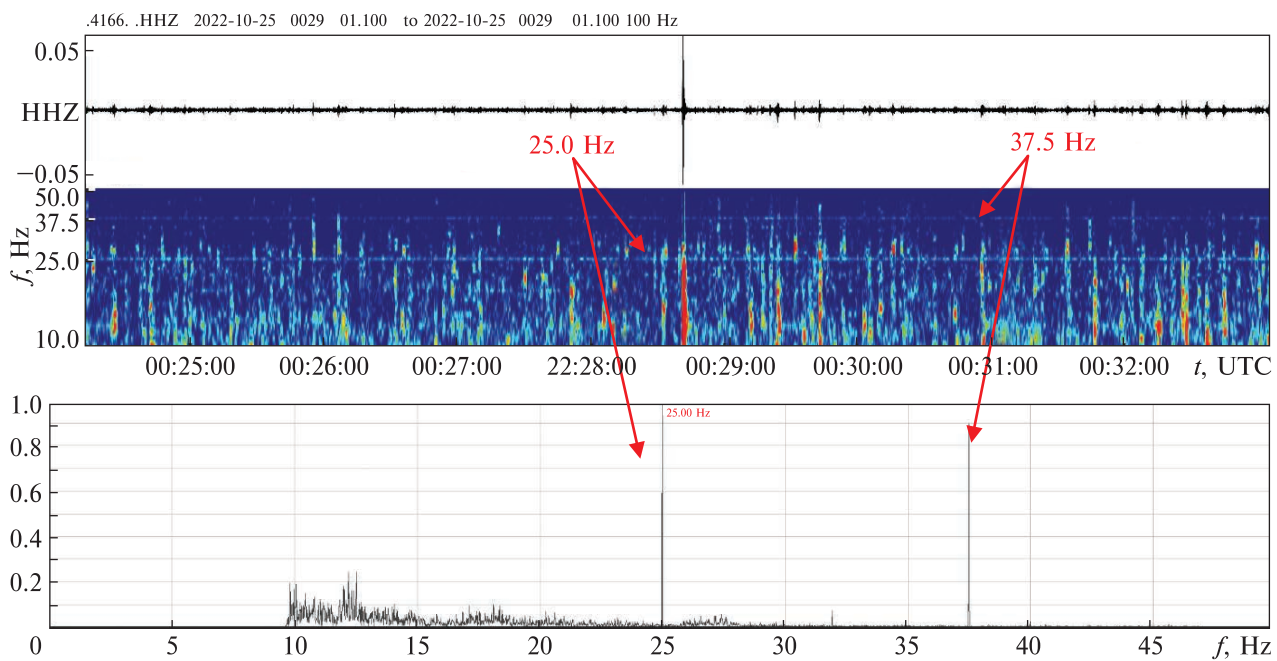


Figure 11. The high-frequency component (10.0–50.0 Hz) of the vertical HHZ component of the seismogram. Time-frequency (logarithmic scale) and amplitude-frequency spectra of the vertical component of the seismic record. Arrows mark harmonics of 25.0 and 37.5 Hz

In addition to fluctuations of ground vibrations caused by natural phenomena, there is also technogenic noise (Fig. 11). Thus, among the random events of a wide high-frequency spectrum, at least two constant harmonics with a frequency of 25.0 and 37.5 Hz stand out on the spectrograms. These harmonics are present over the entire time interval. At the moment, we are unable to explain their origin. They are probably related to a working electric current generator or several mechanical devices.

3 Results

The analysis of seismic records obtained at the Akademik Vernadsky station during 2022–2023 made it possible to select the most typical seismograms of earthquakes with epicenters in geographically different seismic zones. The most seismically active are the Shetland and Sandwich plates and the place where the Nazca plate joins South America. The hypocenters of the selected

earthquakes, respectively, were located in subduction zones at different depths of 10, 78, and 236 km. The distances between the seismic station Guralp CMG 40-TDE of the Akademik Vernadsky station and the epicenters of earthquakes were 325, 2013, and 5620 km, respectively. Polarization analysis was used to determine the onset time of seismic waves (first arrivals) from earthquakes and their type (Pinnegar, 2006; Greenhalgh et al., 2018; Brinkman et al., 2023). The longitudinal P (compression) waves, transverse S waves (shear waves), and Rayleigh and Love (surface) waves were isolated. The methods of time-frequency and amplitude-frequency filtering in a given spatial frequency domain were used to separate seismic oscillations into events of tectonic and non-tectonic origin. Figure 12 displays a four-minute interval with a surface wave in the low-frequency range of 0.001–0.05 Hz without local seismic events.

Glacier ice is a viscoelastic material during long-term action of potential energy and fragility dur-

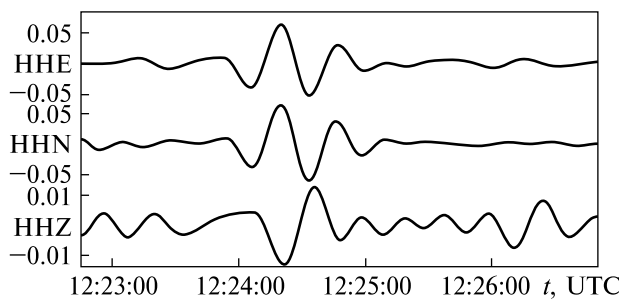


Figure 12. A filtered section of a three-dimensional recording of a surface wave in the range of 0.001–0.05 Hz, registered at the Akademik Vernadsky station from the Peruvian earthquake. The vertical scale is the amplitude of the oscillation of the Earth's surface at the point of observation (in millimeters), and the horizontal scale is the time of registration of seismic waves

ing rapid deformation. High-amplitude oscillations of the Earth's surface in the horizontal and vertical planes, caused by Rayleigh and Love surface waves, contribute to the formation of fractured zones in the glacier due to compression-decompression volumetric movements. In addition, earthquakes with strong surface waves activate their mobility and accelerate the destruction of the continent's ice sheet.

Peng et al. (2014) and Camelbeeck et al. (2017) recorded a number of icequakes immediately after the arrival of long-period surface seismic waves. In particular, during the Chilean earthquake of 2010 (magnitude 8.8), 12 icequakes occurred within four minutes with a gradual decrease in their energy.

Analysing the high-frequency components of the seismic records of the Peruvian earthquake, we found that the induced cryoseismic events showed a high similarity of signal forms with the forms detected at the HOWD station during the POLENET international project (Peng et al., 2014). Also, the impulses associated with cryoseismic events occurred when the recorded ground acceleration (subjected to a surface wave) approached the maximum. In Figure 13, the seismogenic ice fracturing is in the time limits of 12:24:00.160 – 12:24:17.800 UTC. During this time, five high-frequency pulses were registered. The intervals between them, considering transient processes, are

practically the same and roughly correspond to three seconds. The number of pulses and the time between them show a certain regularity. After the passage of the surface wave ($t = 12:25:24.810$), the high-frequency component of the seismogram (Fig. 13) shows an increased number of intense seismic events caused by the further destruction of the ocean ice cover on the coastline and mechanical ablation of the marginal parts of the glacier. These events occur chaotically and have different energy and frequency compositions.

To detect the cryoseismic events, we did a spectral analysis of selected records (i.e., the frequency composition of natural and technogenic noises) during earthquakes and the frequency composition of natural non-tectonic waves and seismic events (including those generated by meteorological factors) and records of probably anthropogenic nature.

4 Discussion

Advanced automatic and visual control methods have been developed to determine the impact of earthquakes on objects on the Earth's surface (Gryn, 2023). Several problems need to be solved to establish the impact of earthquakes on Antarctic glaciers. They are mostly related to the need to simultaneously use a lot of seismic equipment to determine the magnitude of an earthquake in a certain area and monitor the processes in glaciers as high-amplitude waves pass through them. It is possible to identify patterns in cryoseismic phenomena only with long-term observations. This type of seismic data is usually accumulated episodically during international projects, such as POLENET (Lough et al., 2011; Peng et al., 2014). Searching for the cryoseismic events associated with cracks' formation at the Akademik Vernadsky station is complicated because there is only one seismic station on the rocks of Galindez Island. With just one observation point, we discovered interrelated phenomena – the arrival of surface waves and cryoseismic events, which we interpret as triggered by the arriving surface waves.

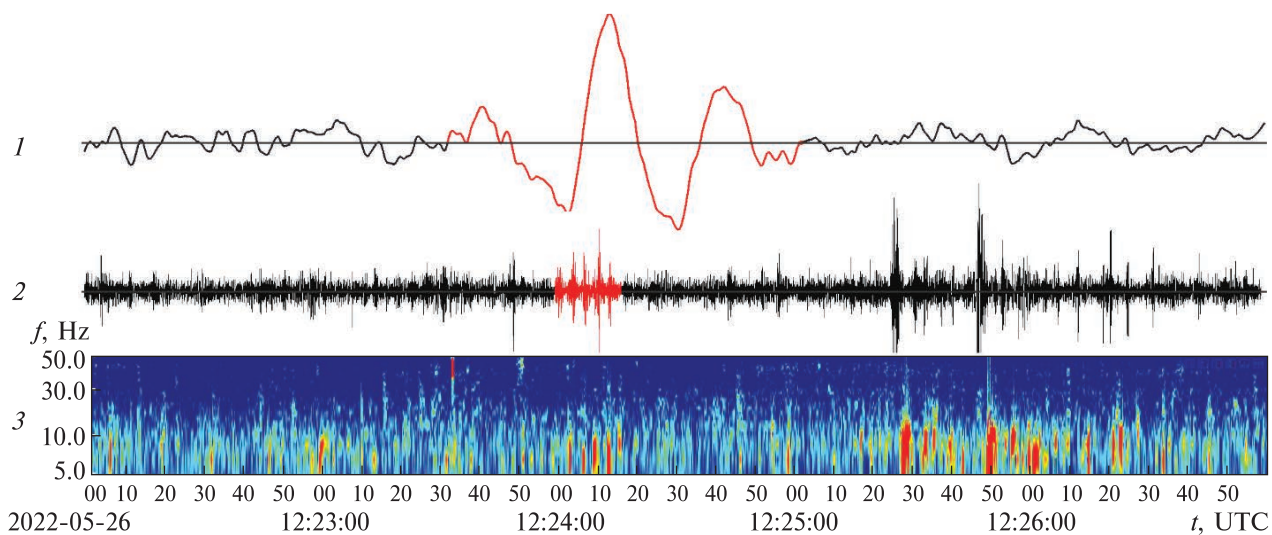


Figure 13. The vertical component of the NSE seismogram with the surface wave of the Peruvian earthquake. 1 – low-frequency component of the seismogram (0–5.0 Hz). The surface wave is marked in red. 2 – high-frequency component (5.0–50.0 Hz). Cryoseismic pulses that occur during the formation of cracks are marked in red. 3 – time-frequency spectrum of the high-frequency component of the seismogram on a logarithmic scale

However, we cannot exactly pinpoint where the event took place; we can only find the approximate radius of its location. The cryoseismic event, which we interpret to be the initiation or growth of surface cracks, did not occur under the seismic station but at some distance from it. Therefore, the recorded amplitude of these oscillations is smaller than at the source. The approach of studying seasonal glacial seismicity by one station located on the surface of glaciers and determining the approximate location of the source of seismicity is described by Köhler et al. (2019). It assumes the homogeneity of the seismic station's environment on a glacier and the absence of chaotic disturbances.

The location of the station near the coastline makes it difficult to detect and identify the arrival times of the first waves and their types. The main reason is the presence of long-term microseisms observed throughout the year. Microseisms mainly occur during stormy weather with winds blowing towards the coast. Oceanic waves and storms form seismic waves with low-frequency harmonics, variable intensity of oscillation, and duration from hours to several days. Usually, they

generate seismic noises with a larger amplitude and are in the low-frequency range, characteristic of earthquake signals. Ice cover complicates removing such interference from seismic data, as it is an additional chaotic source of complex noises (Taylor et al., 2008; Liashchyk & Karyagin, 2018). The role of Rayleigh and Love surface waves in activating glacier seismicity has yet to be determined. However, based on their polarization, we infer that Rayleigh waves promote ice fracturing (horizontal movements), and Love waves make the glaciers move with the harmonic vertical movements of the ground surface (a motion type that may weaken the contact between the glacier ice and underlying geologic materials).

5 Conclusions

The seismic records of the Guralp CMG 40-TDE velocimeter obtained during the wintering of the 27th Ukrainian Antarctic Expedition (2022–2023) were analysed, and the most characteristic seismograms were selected to determine the types of seismic events that are registered at the station and suggest the impact of seismic waves on local glaciers.

The strongest and most influential are the seismic fluctuations of the ground surface, which are associated with strong subduction zone earthquakes. According to the USGS (United States Geological Survey), more than 2000 earthquakes occurred during the winter, located up to 6000 km from Galindez Island and with a moment magnitude greater than four. For the Antarctic Peninsula, three seismically active subduction zones are the most impactful – the Shetland and Sandwich plates and the junction of the Nazca plate with South America (Peruvian-Chilean earthquakes).

The high-amplitude oscillations of the ground surface on which glaciers are located promote ice fracturing. Strong surface waves may also influence glacier sliding and iceberg calving. As indicated by our data, the most impactful surface waves arise from the Peruvian-Chilean earthquakes. Under the influence of surface waves in glaciers, volumetric compression/decompression may lead to ice cracking and associated seismic signals. Such high-frequency oscillations were detected when the surface wave generated by the 2010 Maule earthquake in Chile passed through Galindez Island. These high-frequency events have very similar amplitude-frequency composition, oscillation amplitude, and duration. Thus, they have common features, implying regularities in the reaction of the ice mass to the forcing of surface waves.

The natural movement of glaciers in the vicinity of our Antarctic station causes less noticeable seismic signals. However, the number and intensity of such seismic events significantly increase due to seismic waves created by earthquakes.

The relationship between the many powerful earthquakes and the annual decrease in the ice cover of the western part of Antarctica can be established given a technique for identifying cryo-seismic events originating in and below glaciers using long-term monitoring and additional seismic sensors.

Author contributions: Idea, conceptualization: D. G.; data collection and preparation: O. L., Y. O., Y. A.; research: D. G., O. L.; visualization: D. G.;

manuscript writing: D. G., O. L., Y. O., Y. A. Authors have read and agreed to the final version of the manuscript.

Acknowledgments. The authors thank the State Institution National Antarctic Scientific Center of the Ministry of Education and Science of Ukraine for providing primary data and materials obtained at the Ukrainian Antarctic Akademik Vernadsky station during the 27th Ukrainian Antarctic Expedition (2022–2023).

Funding. This study was performed and partially funded under the State Special-Purpose Research Program in Antarctica for 2011–2025.

Conflict of Interest. The authors declare no conflict of interest.

References

- Anthony, R. E., Aster, R. C., Wiens, D., Nyblade, A., Anandakrishnan, S., Huerta, A., Winberry, J. P., Wilson, T., & Rowe, C. (2015). The seismic noise environment of Antarctica. *Seismological Research Letters*, 86(1), 89–100. <https://doi.org/10.1785/0220140109>
- Aster, R. C., & Winberry, J. P. (2017). Glacial seismology. *Reports on Progress in Physics*, 80(12), 126801. <https://doi.org/10.1088/1361-6633/aa8473>
- Båth, M. (1974). *Spectral Analysis in Geophysics*. Elsevier.
- Brinkman, N., Sollberger, D., Schmelzbach, C., Stähler, S. C., & Robertsson, J. (2023). Applications of time-frequency domain polarization filtering to InSight seismic data. *Earth and Space Science*, 10(11), 1–17. <https://doi.org/10.1029/2023EA003169>
- Camelbeeck, T., Lombardi, D., Collin, F., Rapagnani, G., Martin, H., & Lecocq, T. (2017). Contribution of the seismic monitoring at the Belgian Princess Elisabeth base to East Antarctica ice sheet dynamics and global seismicity studies. *Bulletin des Séances de Académie Royale des Sciences d'Outre-Mer*, 63(2017-1), 163–178. <https://doi.org/10.5281/zenodo.3693877>
- Cannata, A., Larocca, G., Del Carlo, P., Giudice, G., Giuffrida, G., Liuzzo, M., Zuccarello, L., Di Grazia, G., Gambino, S., Privitera, E., Delladio, A., & Grigioni, P. (2017). Characterization of seismic signals recorded in Tethys Bay, Victoria Land (Antarctica): data from atmosphere-cryosphere-hydrosphere interaction. *Annals of Geophysics*, 60(5), S0555. <https://doi.org/10.4401/ag-7408>
- Civile, D., Lodolo, E., Vuan, A., & Loreto M. F. (2012). Tectonics of the Scotia–Antarctica plate boundary constrained from seismic and seismological data. *Tectono-*

- physics*, 550–553, 17–34. <https://doi.org/10.1016/j.tecto.2012.05.002>
- Davison, B. J., Hogg, A. E., Gourmelen, N., Jakob, L., Wuite, J., Nagler, T., Greene, C. A., Andreasen, J., & Engdahl, M. E. (2023). Annual mass budget of Antarctic ice shelves from 1997 to 2021. *Science Advances*, 9, 1–12. <https://doi.org/10.1126/sciadv.adl0186>
- Feeenstra, J., Hull, A., Li, F., Fraser, J., Howard, M., & McMorrin, T. (2019). Estimating seismic hazard with Sparse Data: Seismic source model and sensitivity of a PSHA for Palmer Station, Antarctica. *2019 Pacific Conference on Earthquake Engineering and Annual NZSEE Conference*, 4–6 April 2019, New Zealand.
- Giner-Robles, J. L., Pérez-López, R., Rodríguez-Pascua, M. A., Martínez-Díaz, J. J., & González-Casado, J. M. (2009). Present-day strain field on the South American slab underneath the Sandwich Plate (Southern Atlantic Ocean): A kinematic model. *Geological Society, London, Special Publications*, 328(1), 155–167. <https://doi.org/10.1144/SP328.6>
- Govers, R., Broerse, T., & Herman, M. (2021). Tectonic context of the August 2021 South Sandwich Islands earthquake sequence: plate boundary geometry and kinematics at active STEPs. *AGU Fall Meeting 2021*, New Orleans, LA, 13–17 December 2021. <https://doi.org/10.1002/essoar.10509096.1>
- Greenhalgh, S., Sollberger, D., Schmelzbach, C., & Rutty, M. (2018). Single-station polarization analysis applied to seismic wavefields: A tutorial. *Advances in Geophysics*, 59, 123–170. <https://doi.org/10.1016/bs.agph.2018.09.002>
- Gryn, D. (2023). Seismic hazard of the territory of Ukraine: according to the materials of scientific report at the meeting of the Presidium of NAS of Ukraine, March 8, 2023. *Visnyk of the National Academy of Sciences of Ukraine*, (6), 25–33. <https://doi.org/10.15407/vishn2023.06.025>
- Jennings, S. J. A., & Hambrey, M. J. (2021). Structures and deformation glaciers and ice sheets. *Reviews of Geophysics*, 59, e2021RG000743. <https://doi.org/10.1029/2021RG000743>
- Jia, Z., Zhan, Z., & Kanamori, H. (2022). The 2021 South Sandwich Island M_w 8.2 earthquake: a slow event sandwiched between regular ruptures. *Geophysical Research Letters*, 49(3), e2021GL097104. <https://doi.org/10.1029/2021GL097104>
- Köhler, A., Maupin, V., Nuth, C., & van Pelt, W. (2019). Characterization of seasonal glacial seismicity from a single-station on-ice record at Holtedahlfonna, Svalbard. *Annals of Glaciology*, 60(79), 23–36. <https://doi.org/10.1017/aog.2019.15>
- Li, C., Peng, Z., Chaput, J. A., Walter, J. I., & Aster, R. C. (2021). Remote triggering of icequakes at Mt. Erebus, Antarctica by large teleseismic earthquakes. *Seismological Research Letters*, 92(5), 2866–2875. <https://doi.org/10.1785/0220210027>
- Li, W., Chen, J., Lu, H., Yu, C., Shan, Y., Li, Z., Dong, X., & Xu, Q. (2023). Analysis of seismic impact on Hailuogou Glacier after the 2022 Luding Ms 6.8 earthquake, China, using SAR offset tracking technology. *Remote Sensing*, 15, 1468. <https://doi.org/10.3390/rs15051468>
- Li, Z., Sun, J., Gao, M., Fu, G., An, Z., Zhao, Y., Fang, L., & Guo, X. (2022). Evaluation of horizontal ground motion waveforms at Sedongpu Glacier during the 2017 M6.9 Mainling earthquake based on the equivalent Green's function. *Engineering Geology*, 306, 106743. <https://doi.org/10.1016/j.enggeo.2022.106743>
- Liashchuk, O. I., & Karyagin, Ye. V. (2018). Features of seismicity in the Argentine Islands Archipelago region due to the processes of icebergs formation. *Ukrainian Antarctic Journal*, (1(17)), 32–39. [https://doi.org/10.33275/1727-7485.1\(17\).2018.29](https://doi.org/10.33275/1727-7485.1(17).2018.29)
- Liu, Q., Zhang, B., Zhao, B., Zhong, Y., Lu, X., & Zhou, J. (2022). Stability of the Hailuogou glacier during the “9.5” Luding Earthquake: a preliminary assessment based on multi-source observations. *Journal of Mountain Science*, 19, 3037–3050. <https://doi.org/10.1007/s11629-022-7730-x>
- Lough, A. C., Barchek, C. G., Wiens, D. A., Barklage, M. E., Nyblade, A., Aster, R. C., Anandakrishnan, S., Huerta, A. D., & Wilson, T. J. (2011). Detection of seismic sources associated with ice movement in Antarctica using POLENET seismic array, AGAP seismic array, and GSN seismic stations. *AGU Fall Meeting 2011*, id. C41D-0433.
- McBrearty, I. W., Zoet, L. K., & Anandakrishnan, S. (2020). Basal seismicity of the Northeast Greenland Ice Stream. *Journal of Glaciology*, 66(257), 430–446. <https://doi.org/10.1017/jog.2020.17>
- Paolo, F. S., Fricker, H. A., & Padman, L. (2015). Volume loss from Antarctic ice shelves is accelerating. *Science*, 348(6232), 327–331. <https://doi.org/10.1126/science.aaa0940>
- Peng, Z., Walter, J. I., Aster, R. C., Nyblade, A., Wiens, D. A., & Anandakrishnan, S. (2014). Antarctic icequakes triggered by the 2010 Maule earthquake in Chile. *Nature Geoscience*, 7(9), 677–681. <https://doi.org/10.1038/ngeo2212>
- Pinnegar, C. R. (2006). Polarization analysis and polarization filtering of three-component signals with the time-frequency S transform. *Geophysical Journal International*, 165(2), 596–606. <https://doi.org/10.1111/j.1365-246X.2006.02937.x>
- Reading, A. M. (2007). The seismicity of the Antarctic plate. In S. Stein, & S. Mazzotti, *Continental Intraplate Earthquakes: Science, Hazard, and Policy Issues* (pp. 285–298). *Geological Society of America*. [https://doi.org/10.1130/2007.2425\(18\)](https://doi.org/10.1130/2007.2425(18))

- Ringler, A. T., Anthony, R. E., Aster, R. C., Ammon, C. J., Arrowsmith, S., Benz, H., Ebeling, C., Frassetto, A., Kim, W.-Y., Koelmeijer, P., Lau, H. C. P., Lekić, V., Montagner, J. P., Richards, P. G., Schaff, D. P., Vallée, M., & Yeck, W. (2022). Achievements and prospects of global broadband seismographic networks after 30 years of continuous geophysical observations. *Reviews of Geophysics*, 60, e2021RG000749. <https://doi.org/10.1029/2021RG000749>
- Schepers, G., van Hinsbergen, D. J. J., Spakman, W., Kosters, M. E., Boschman, L. M., & McQuarrie, N. (2017). South-American plate advance and forced Andean trench retreat as drivers for transient flat subduction episodes. *Nature Communications*, 8, 15249. <https://doi.org/10.1038/ncomms15249>
- Smalley, R., Bevis, M., & Dalziel, I. (2021). Tectonic setting of the 2021 earthquake doublet in the South Sandwich-South America convergent plate boundary system. *AGU Fall Meeting 2021*, New Orleans, LA, 13–17 December 2021, id. S42C-07.
- Stein, S., Engeln, J. F., DeMets, C., Gordon, R. G., Woods, D., Lundgren, P., Argus, D., Stein, C., & Wiens, D. A. (1986). The Nazca-South America convergence rate and the recurrence of the Great 1960 Chilean Earthquake. *Geophysical Research Letters*, 13(8), 713–716. <https://doi.org/10.1029/GL013i008p00713>
- Su, Y., & Liu, E. I. (2019). Numerical simulation of dynamic analysis of glacier under seismic loading based on combined finite-discrete method. *IOP Conference Series: Earth and Environmental Science*, 283, 012064. <https://doi.org/10.1088/1755-1315/283/1/012064>
- Sykes, L. R. (2021). Decadal seismicity before great earthquakes—strike-slip faults and plate interiors: major asperities and low-coupling zones. *International Journal of Geosciences*, 12(9), 784–833. <https://doi.org/10.4236/ijg.2021.129044>
- Taylor, F. W., Bevis, M. G., Dalziel, I. W. D., Smalley Jr., R., Frohlich, C., Kendrick, E., Foster, J., Phillips, D., & Gudipati, K. (2008). Kinematics and segmentation of the South Shetland Islands-Bransfield basin system, northern Antarctic Peninsula. *Geochemistry, Geophysics, Geosystems*, 9(4), 1–7. <https://doi.org/10.1029/2007GC001873>
- Tsuboi, S., Kikuchi, M., Yamanaka, Y., & Kanao, M. (2000). The March 25, 1998 Antarctic Earthquake: Great earthquake caused by postglacial rebound. *Earth, Planets and Space*, 52, 133–136. <https://doi.org/10.1186/BF03351621>
- van de Lagemaat, S. H. A., Swart, M. L. A., Vaes, B., Kosters, M. E., Boschman, L. M., Burton-Johnson A., Bijl, P. K., Spakman, W., & van Hinsbergen, D. J. J. (2021). Subduction initiation in the Scotia Sea region and opening of the Drake Passage: When and why? *Earth – Science Reviews*, 215, 1–25, 103551. <https://doi.org/10.1016/j.earscirev.2021.103551>
- Walter, J. I., Peng, Z., Tulaczyk, S. M., & Oneil, S. (2013). Triggering of glacier seismicity (icequakes) by distant earthquakes. *American Geophysical Union, Spring Meeting 2013*, id. C24A-02
- Wang, Y. (2022). *Time-frequency analysis of seismic signals*. John Wiley & Sons, Ltd. <https://doi.org/10.1002/9781119892373>
- Xie, J., Zeng, X., Liang, C., Ni, S., Chu, R., Bao, F., Lin, R., Chi, B., & Lv, H. (2024). Ice plate deformation and cracking revealed by an in situ-distributed acoustic sensing array. *The Cryosphere*, 18, 837–847. <https://doi.org/10.5194/tc-18-837-2024>
- Yegorova, T., Bakhmutov, V., Janik, T., & Grad, M. (2011). Joint geophysical and petrological models for the lithosphere structure of the Antarctic Peninsula continental margin. *Geophysical Journal International*, 184(1), 90–110. <https://doi.org/10.1111/j.1365-246X.2010.04867.x>

Received: 21 May 2024

Accepted: 9 January 2025

Дмитро Гринь^{1,*}, Олександр Ляшук², Юрій Отруба³, Юрій Андрушченко²

¹ Інститут геофізики ім. С.І. Субботіна НАН України, м. Київ, 03142, Україна

² Головний центр спеціального контролю НЦУВКЗ ДКА України,
смт. Городок, Житомирська обл., 12265, Україна

³ Державна установа Національний антарктичний науковий центр МОН України,
м. Київ, 01601, Україна

* Автор для кореспонденції: gryn.dmytro@ukr.net

Вплив поверхневих хвиль південноамериканських землетрусів на льодовиковий покрив Антарктичного півострова

Реферат. Землетруси породжують коливання поверхні геологічного середовища, яке має руйнівний ефект для льодовикового покриву Антарктиди. У результаті взаємодії сейсмічних хвиль з льодовиком в ньому з'являється додаткова тріщинуватість, підвищується його рухливість та текучість. Ці процеси пришвидшують змен-

шення загальної маси льодового покриву західної Антарктиди. Метою публікації є аналіз фізичного впливу на льодовики землетрусів, які були зареєстровані на антарктичній станції «Академік Вернадський», та опосередкованого виявлення наслідків руйнування цілісної структури льодовика, які супроводжуються появою викликаної сейсмічності. Для аналізу реакції льодової товщі на землетрус були відібрані найбільш характерні хвильові поля від різних сейсмічно активних зон навколо о. Галіндез. Проведено аналіз прискорення поверхні ґрунту для короткочасних землетрусів та часу, впродовж якого льодовики знаходилися під впливом коливних явищ. Щоб уникнути сумарного ефекту від поперечних, повздовжніх та поверхневих хвиль були використані сейсмічні дані від максимально віддаленого Перуанського землетрусу з магнітудою 7.2, який відбувся 2022-05-26 о 12:02:21 UTC. Сейсмічні хвилі різних типів приходять у точку спостереження у різний час через велику відстань та різну швидкість розповсюдження хвиль. Це виокремлює їх у часі, що дозволяє вивчати взаємодію кожного типу хвилі і льодовика. В публікації проаналізовано дію довгоперіодної поверхневої хвилі на товщу острівних льодовиків, які знаходяться на невеликій відстані від о. Галіндез. Встановлено, що викликана кріосейсмічність проявляється у високочастотній області сейсмічних записів низкою імпульсів, які пов'язують з утворенням тріщин та розломів у льодовиках. Використовувались дані сейсмостанції Guralp CMG 40-TDE, єдиної на території антарктичної станції «Академік Вернадський». Наявні сейсмічні дані дозволили виявити причинно-наслідковий зв'язок землетрусів та кріосейсміки, однак не дозволяють визначити просторове розташування виявлених подій. Проведено аналіз хвильових полів-завад, які характерні для о. Галіндез та ускладнюють процедуру виявлення цільових (поверхневих) хвиль.

Ключові слова: кріосейсміка, льодовики, магнітуда, сейсмологія